

# Proximal Tubular Expression Patterns of Megalin and Cubilin in Proteinuric Nephropathies



Jia Sun<sup>1</sup>, Kjell Hulthenby<sup>2</sup>, Jonas Axelsson<sup>3,4</sup>, Johan Nordström<sup>5,6</sup>, Bing He<sup>3</sup>, Annika Wernerson<sup>1,7,9</sup> and Karin Lindström<sup>1,8,9</sup>

<sup>1</sup>Division of Renal Medicine, Department of Clinical Science, Intervention and Technology, Karolinska Institutet, Stockholm, Sweden; <sup>2</sup>Division of Clinical Research Center, Department of Laboratory Medicine, Karolinska Institutet, Stockholm, Sweden; <sup>3</sup>Division of Matrix Biology, Department of Medical Biochemistry and Biophysics; Karolinska Institutet, Stockholm, Sweden; <sup>4</sup>Department Clinical Immunology, Karolinska University Hospital, Stockholm, Sweden; <sup>5</sup>Division of Transplantation, Department of Clinical Science, Intervention and Technology, Karolinska Institutet, Stockholm, Sweden; <sup>6</sup>Department of Transplant Surgery, Karolinska University Hospital, Stockholm, Sweden; <sup>7</sup>Department of Pathology, Karolinska University Hospital, Stockholm, Sweden; and <sup>8</sup>Department of Nephrology, Karolinska University Hospital, Stockholm, Sweden

**Introduction:** Receptor-mediated endocytosis is responsible for protein reabsorption in the proximal tubules. For albumin this process involves at least 2 interacting receptors, megalin and cubilin. Albumin is not usually present in the urine, indicating a highly efficient tubular reuptake under physiological conditions. However, early appearance of albuminuria may mean that the tubular system is overwhelmed by large quantities of albumin or that the function is impaired.

**Methods:** To better understand the physiological role of megalin and cubilin in human renal disease, renal biopsies from 15 patients with a range of albuminuria and 3 healthy living donors were analyzed for proximal tubular expression of megalin and cubilin using immunohistochemistry (IHC) and semi-quantitative immune-electron microscopy. Their expression in proteinuric zebrafish was also studied.

**Results:** Megalin and cubilin were expressed in brush border and cytoplasmic vesicles. Patients with microalbuminuric IgA nephropathy and thin membrane disease had significantly higher megalin in proximal tubules, whereas those with macro- or nephrotic-range albuminuria had unchanged levels. Cubilin expression was significantly higher in all patients. In a proteinuric zebrafish nphs2 knockdown model, we found a dose-dependent increase in the expression of tubular megalin and cubilin in response to tubular protein uptake.

**Discussion:** Megalin and cubilin show different expression patterns in different human diseases, which indicates that the 2 tubular proteins differently cooperate in cleaning up plasma proteins in kidney tubules.

*Kidney Int Rep* (2017) 2, 721–732; <http://dx.doi.org/10.1016/j.ekir.2017.02.012>

KEYWORDS: albuminuria; cubilin; megalin; proximal tubule

© 2017 International Society of Nephrology. Published by Elsevier Inc. This is an open access article under the CC BY-NC-ND license (<http://creativecommons.org/licenses/by-nc-nd/4.0/>).

Megalin<sup>1</sup> (also known as Lrp2, low-density lipoprotein-related protein 2) and cubilin<sup>2</sup> are 2 large transmembrane proteins expressed on the surface of proximal tubular epithelial cells, where they are central to the endocytic reabsorption of many plasma proteins filtered across the glomerular capillary wall.<sup>3–6</sup> This mechanism is evolutionarily conserved and exists also in zebrafish.<sup>7</sup>

Under a normal physiological condition, some albumin molecules pass through the glomerular filtration barrier<sup>8,9</sup> but are reabsorbed by the proximal tubular epithelium.<sup>10</sup> Consequently, albumin is not present in the urine of healthy individuals, and the presence of minute amounts of protein is considered as a sensitive marker of a dependent risk factor for future progression of renal disease.<sup>11</sup> The mechanism behind these observations is unclear, but increasing the load of protein taken up and recycled by the proximal tubular cells potentially contributes to the development of inflammation and fibrosis.<sup>12</sup>

In proteinuric diseases such as IgA nephropathy (IgAN) and minimal change nephrotic syndrome, large amounts of plasma proteins, including albumin, enter

**Correspondence:** Karin Lindström, M-99, Karolinska University Hospital, Renal Medicine, Stockholm 141 86, Sweden. E-mail: [karin.lindstrom@SLL.se](mailto:karin.lindstrom@SLL.se)

<sup>9</sup>These authors contributed equally to this work.

Received 20 June 2016; revised 9 February 2017; accepted 21 February 2017; published online 1 March 2017

the tubules.<sup>13</sup> However, the role of megalin and cubilin<sup>14</sup> is unclear. Despite multiple studies reported in cells,<sup>15–17</sup> mice,<sup>18–21</sup> rats,<sup>22,23</sup> and dogs,<sup>24,25</sup> very little is known about the role of megalin and cubilin in humans.<sup>26,27</sup> Available data rely on the phenotypes of rare genetic diseases resulting in dysfunctional megalin (Dent's disease,<sup>28–30</sup> Lowe's syndrome,<sup>28,29</sup> and Donnai-Barrow syndrome<sup>5,31–34</sup>) or cubilin (Imerslund–Gräsbeck syndrome<sup>35–38</sup> and Fanconi-bichel syndrome<sup>39</sup>). However, it remains unclear how normal megalin and cubilin respond to increased protein load in common human kidney diseases.

We hypothesized that the expression of proximal tubular megalin and cubilin may correlate to the degree of albuminuria. In this study, we used human kidney biopsies from albuminuric nephropathies to study the subcellular localization and the role of megalin and cubilin in patients with albuminuria of different degree. As controls, we used healthy kidney donor biopsies. Furthermore, a proteinuric zebrafish model was used to confirm our findings.

## MATERIALS AND METHODS

### Ethical Statement

Approval was obtained from the Ethical Committee in Stockholm, Sweden, before the initiation of the study.

### Patients

This study included a cohort of 15 patients (mean age 30 years, 10 patients are male) with kidney diseases selected from incident patients who underwent diagnostic renal biopsy at the Karolinska University Hospital between 2000 and 2013. We chose IgAN with different degrees of albuminuria and compared the results with a disease resulting in nephrotic-grade albuminuria and one nonalbuminuric (thin membrane disease, TMD). We also classified the patients according to the albuminuric levels. Group 1: albuminuria <300 mg/24 hours group: TMD (nonalbuminuric, n = 3) and microalbuminuric IgAN (>30 mg/24 hours and <300 mg/24 hours, n = 3);<sup>40,41</sup> group 2: albuminuria >300 mg/24 hours and <3500 mg/24 hours group: macro-albuminuric IgAN (n = 3);<sup>41</sup> group 3: albuminuria >3500 mg/24 hours group: nephrotic-albuminuric IgAN (n = 3) and minimal change nephrotic syndrome (n = 3). Biopsies from 3 healthy living kidney donors were used as controls. These biopsies were taken immediately after removal of the kidney from the donor and before flushing with preservative solution. All patients' characteristics are shown in [Table 1](#).

### Kidney Biopsies

For light microscopy, the specimens were fixed in 4% phosphate buffered formalin, and then dehydrated and

embedded in paraffin according to standard procedures. Sections of 1.5 µm were cut on a microtome and stained with hematoxylin and eosin, periodic-acid Schiff, Ladewig's trichrome, and periodic acid silver. Materials for diagnostic transmission electron microscopy were fixed in a mix of 2.5% glutaraldehyde and 0.5% paraformaldehyde and embedded in an epoxy resin. The blocks were cut into approximately 60-nm-thick sections and evaluated under a transmission electron microscope.

The histopathology of the included patients' biopsies was re-examined by an experienced nephropathologist to confirm the respective diagnoses. Tubular atrophy and interstitial fibrosis were semi-quantified according to Banff criteria.<sup>32</sup> Thus, tubular atrophy was graded between 0 and 3: 0 = none, 1 = affecting 0 to 25% of the cortical area, 2 = affecting 26% to 50%, and 3 = affecting >50%. Interstitial fibrosis was graded 0–3: 0 = affecting 0 to 5% of the cortical area, 1 = affecting 6% to 25%, 2 = affecting 26% to 50%, and 3 = affecting >50%.

### Biochemical Methods

Biochemical analyses were performed on serum albumin, serum creatinine, and albuminuria using routine methods at the Department of Clinical Chemistry, Karolinska University Hospital at Huddinge.

### Generation of Proteinuric Zebrafish

The proteinuric zebrafish model was generated by morpholino-mediated knocking down of *nphs2* as described earlier.<sup>42</sup> The morpholino antisense oligo (MO) targeting *nphs2* (5'-TAGACTTACCTTCTCCAGGTCCCTC) and a standard control MO (5'-CCTCTTACCTCAGTTACAATTTATA) were obtained from GENE TOOLS, LLC, Philomath, OR. Two doses (50 µM and 100 µM) of *nphs2* MO were injected into 1- or 2-cell embryos, respectively. As a control, 100 µM of control MO was used for injection. In general, 2 nl of MO solution with the concentrations above was microinjected into the yolk of an embryo. In the knockdown experiments, we used embryos from a wild-type AB zebrafish line, which is maintained and raised in the zebrafish core facility, Karolinska Institute, as described.<sup>43</sup> In the larval stage, *nphs2* knockdown in zebrafish is unlikely to lead to human-like massive proteinuria due to a relatively low level of plasma proteins. It has been shown that albumin appears to be absent in zebrafish plasma due to the lack of the gene encoding albumin in its genome, but instead a plasma vitamin D binding protein, which may have a similar function to albumin in zebrafish,<sup>44</sup> exists and shows 40% homology (amino acid similarity by the Blast comparison) of mammalian albumin. An antibody

**Table 1.** Patients' clinical and biochemical characteristics

No.	Diagnosis	Age (yr)	Gender (male = 1)	S-Alb (g/l)	S-Crea ( $\mu\text{mol/l}$ )	U-Alb (mg/24 h)	GFR (ml/min)	Tubular atrophy	Interstitial fibrosis
1	Donor	41	0	40	71	26	120	0	1
2	Donor	46	0	38	58	3	108	0	0
3	Donor	34	0	42	84	8	104	0	0
4	TMD	13	0	42	54	4	133	1	0
5	TMD	10	0	43	53	9	143	0	0
6	TMD	47	0	40	80	6	135	1	1
7	micro-IgAN	19	1	42	91	158	82	1	1
8	micro-IgAN	25	0	38	61	58	149	1	1
9	micro-IgAN	26	1	40	69	58	141	1	0
10	macro-IgAN	31	1	36	125	1,499	71	1	0
11	macro-IgAN	48	1	38	107	1,925	123	1	2
12	macro-IgAN	26	1	38	81	1,821	149	1	2
13	nephro-IgAN	17	1	13	66	9,767	157	0	0
14	nephro-IgAN	55	1	17	110	6,938	83	1	1
15	nephro-IgAN	49	1	32	108	4,441	70	1	1
16	MCNS	19	1	10	77	14,762	134	0	0
17	MCNS	29	1	16	62	6,380	75	0	0
18	MCNS	29	0	14	71	4,023	57	1	1

GFR, glomerular filter rate; macro-IgAN, IgA nephropathy with macroalbuminuria; MCNS, minimal change nephrotic syndrome; micro-IgAN, IgA nephropathy with microalbuminuria; nephron-IgAN, IgA nephropathy with nephrotic-albuminuria; S-Alb, serum albumin; S-Crea, serum creatinine; TMD, thin membrane disease; U-Alb, uric albumin.

to full-length rat albumin we used in immunoelectron microscopy (iEM) assay in fact was able to recognize the epitopes of absorbed albumin-like protein, probably vitamin-D binding protein, in proximal tubules of the nphs2 morphants.

Whole embryos were observed using a Leica MZ12 dissecting stereomicroscope with an attached digital camera. Pericardial edema of the morphants was analyzed and photographed at 4 days postfertilization (dpf). For transmission electron microscopy and iEM, 4-dpf morphants were fixed with 3% paraformaldehyde and kept at 4 °C until the next procedure for dehydration and embedding.

## Antibodies

Following light microscopy to determine the integrity and structure of the proximal tubules in each biopsy, we studied human samples using sheep antimegalin and rabbit anticubilin antibodies (gift from Professor Renata Kozyraki, Institute de la Vision, INSERM, Paris, France) as well as rabbit antialbumin antibodies (Sigma, cat. no. A3293-2ML). To detect the signal of reabsorbed protein in larval zebrafish proximal tubules, the sheep anti-full-length-rat albumin antibody (Bethyl Laboratories; cat. no. A110-134A) was used for the iEM analysis. We used the antibodies to megalin (Atlas, cat. no. HPA005980) and cubilin (Biorbyt, cat. no. orb4997) for IHC analysis and zebrafish iEM analysis; the Blast analysis shows that zebrafish homology of the immunogen peptides for megalin and cubilin is 80% of similarity and 83% of similarity, respectively. Normal sheep serum (Dako, cat. no. X 0503) and normal rabbit IgG fraction (Dako, cat. no. X0903) were used as negative controls. To detect bound

antibodies, a secondary gold-conjugated protein A (10 nm) or gold-conjugated donkey anti-sheep (10 nm) antibody (British Biocell International, cat. no. 7687 and 15249) was used.

## Immunohistochemistry

IHC was performed on paraffin sections from all biopsies using the standard IHC protocol in the Department of Pathology and staining was analyzed by using a Bond-III microscope (Leica Biosystem, Wetzlar, Germany). Antibodies to megalin (1:500) and cubilin (1:200) were used.

## Immunoelectron Microscopy

A small piece of each kidney biopsy was collected for iEM. The tissue was fixed in a solution containing 0.1 M phosphate-buffered 1% paraformaldehyde and 0.5% glutaraldehyde and processed for low-temperature embedding into K11M.<sup>45</sup> We used a dilution of 1:100 for megalin antibody, whereas the other 2 antibodies and all secondary antibodies were diluted 1:200. Sections of approximately 70 nm were incubated overnight with the primary antibodies rinsed and bound antibodies were detected with protein A or secondary antibodies for 2 hours. Normal sheep serum and normal rabbit IgG fraction diluted to the same concentration as the corresponding primary antibodies were used as negative controls.

All sections were analyzed under a Tecnai 10 microscope (FEI, Eindhoven, The Netherlands) at 100 kV and digital images were captured with a Veleta camera (Olympus Soft Imaging Solutions GmbH, Münster, Germany).

## Semiquantification of Protein Expression in iEM

To determine the number of images needed for an appropriate sampling, we used a cumulative mean plot as previously described.<sup>46</sup> Thus, in the present study, 10 proximal tubules were chosen randomly and in each tubule 3 different areas were selected. In each area, 1 image at a primary magnification of  $\times 39,000$  covering brush border and 1 image covering the adjacent apical cytoplasmic vesicles were taken (Figure 1). Thus, 30 images were analyzed in each compartment, respectively. The area of the corresponding compartments was calculated by point counting using a  $1 \times 1$  cm square lattice, and expressed as  $\mu\text{m}^2$ .<sup>46</sup> The number of gold particles was counted in the images and the concentration of each protein was calculated by dividing the total number of gold particles by the area, and expressed as gold particles/ $\mu\text{m}^2$  ( $\text{Au}/\mu\text{m}^2$ ). The mean concentration was then calculated in each compartment.

The method described<sup>46</sup> was used to calculate the images of zebrafish samples. Because the zebrafish nephron has only 2 tubuli, 4 consecutive sections were analyzed in each zebrafish tubule, and in each section, 5 areas including brush border and cytoplasmic vesicles were randomly selected. Thus, 20 images were analyzed in each compartment, respectively.

## Statistical Analysis

All variables were expressed as mean and SEM. A  $P$ -value  $<0.05$  was considered to be statistically significant.

Comparisons between 6 groups among patient biopsies and 3 groups among zebrafish biopsies were performed using the general linear model test. All statistical analyses were performed in version 9.4 of the SAS software package (SAS Institute).

## RESULTS

### Patient Characteristics

We have studied common renal diseases with varying degrees of albuminuria. Group 1 (albuminuria  $<300$  mg/24 hours): microalbuminuric IgAN and non-albuminuric TMD; group 2 (albuminuria  $>300$  mg/24 hours and  $<3500$  mg/24 hours): macroalbuminuric IgAN; and group 3 (albuminuria  $>3500$  mg/24 hours): nephrotic-albuminuric IgAN and minimal change nephrotic syndrome.

Both serum ( $P = 0.003$ ) and urinary ( $P = 0.002$ ) albumin differed significantly between the 3 groups. Clinical characteristics of the included patients are given in Table 1. On the basis of our hypothesis, we studied levels of megalin and cubilin in the albuminuria groups shown above, rather than by diagnosis. Semiquantification of tubular atrophy and interstitial fibrosis showed that there was no or limited mild tubular atrophy and no or mild interstitial fibrosis in all biopsies except in 2 patients with IgAN showing moderate interstitial fibrosis (Table 1).

### IHC of Megalin and Cubilin

Staining for megalin and cubilin (Figure 2) showed labeling at different intensities in different structures. The most intense staining was seen in the luminal part of the proximal tubules, and there was background level staining in distal tubules (Figure 2A[a] and B[a]).

As shown for megalin staining in Figure 2A, biopsies from patients with nonalbuminuric TMD and macroalbuminuric IgAN were shown to be more intense (Figure 2A[c] and [e]) compared with others. Compared with megalin, staining for cubilin (Figure 2B) was positive on the luminal side of proximal and background level staining in distal tubules (Figure 2B[a]).

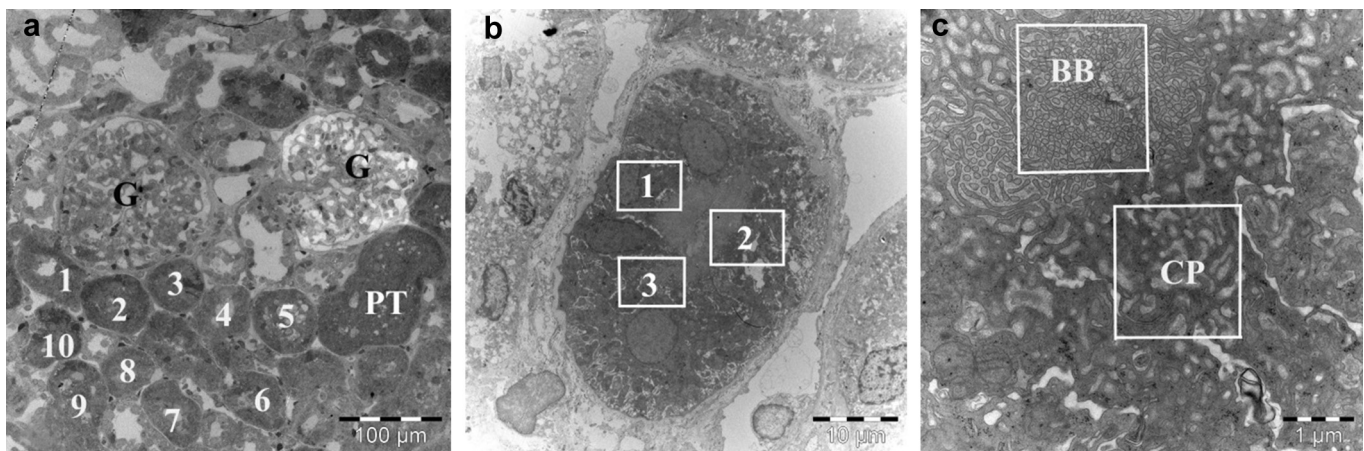


**Figure 1.** Immunoelectron microscope images show the collection of images for the semiquantification in proximal tubules (PT). (a) Ten proximal tubules (1–10) were randomly selected, and (b) in each tubule, 3 different areas (1–3) were randomly selected. (c) In each area, 1 image (original magnification  $\times 39,000$ ), brush border (BB) and adjacent apical cytoplasm area (CP), was taken separately. G, glomerulus.



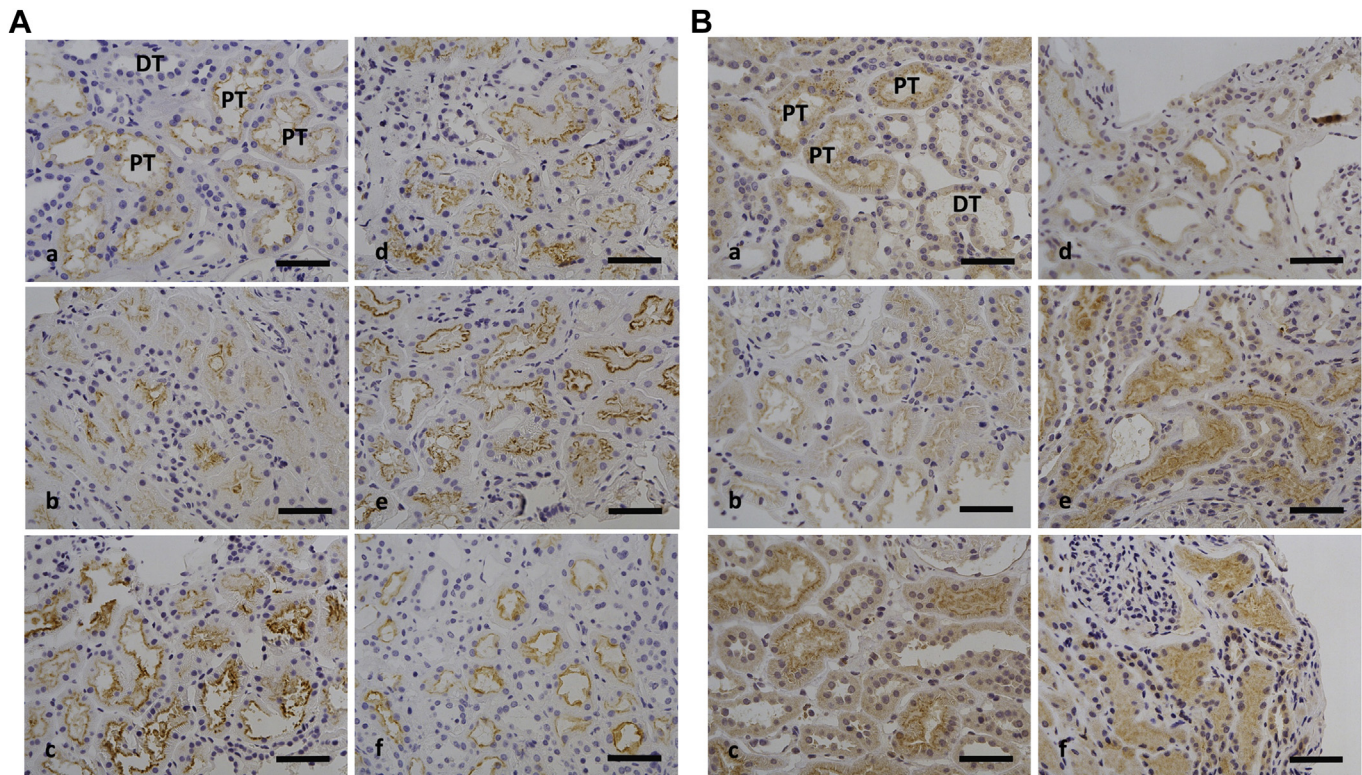


**Figure 2.** Immunohistochemistry staining using antibodies against (A) megalin and (B) cubilin. Biopsies from patients with (a) control, (b) minimal change nephropathy (MCNS), (c) thin membrane disease (TMD), (d) nephrotic-albuminuric IgA nephropathy (IgAN) (>3500 mg/24 hours), (e) macroalbuminuric IgAN (>300 mg/24 hours and <3500 mg/24 hours), and (f) microalbuminuric IgAN (<300 mg/24 hours) show the labeling at different intensities; the most intense staining was observed in the luminal aspect of the proximal tubules (PT), whereas staining of the distal tubules (DT) was at background levels. Bar = 50  $\mu\text{m}$ .

Biopsies from the nonalbuminuric TMD, macroalbuminuric IgAN, and microalbuminuric IgAN groups showed the highest labeling intensity (Figure 2B[c], [e], and [f]), whereas no major differences were found comparing the other biopsies.

### Immunoreactivity in Proximal Tubular Cells Analyzed by iEM

Controls incubated with normal sheep serum showed nonspecific labeling at background levels in both the brush border ( $0.5 \text{ Au}/\mu\text{m}^2$ ) and the cytoplasmic vesicles ( $0.4 \text{ Au}/\mu\text{m}^2$ ). Controls labeled with normal rabbit IgG also showed low nonspecific labeling in both the brush border ( $0.7 \text{ Au}/\mu\text{m}^2$ ) and cytoplasmic vesicles ( $0.7 \text{ Au}/\mu\text{m}^2$ ) likely due to nonspecific binding (data not shown).

The observed quantity of labeled antibody, and thus of immunoreactive megalin and cubilin, differed between diseases, as did the distributions in the proximal tubular epithelium. This is illustrated in Figure 3 (patients biopsies,  $\times 39,000$ ) and Figure 4B (zebrafish samples,  $\times 43,000$ ). In each instance, labeling occurred both in the brush border and cytoplasmic vesicles, whereas the labeling in the tubular lumen did not exceed that of nonspecific background labeling

(Figure 3 and Figure 4B). In the cytoplasm area, labeling was mainly observed in vesicles (Figure 3f).

### Semiquantitative Evaluation of Immunoreactive Megalin and Cubilin in Human Proximal Tubular Cells Using iEM

Semiquantification data are summarized in Figure 5 shown in 2 models: Figure 5A and B are classified by diagnosis, and Figure 5C and D are classified by degree of albuminuria. In both the brush border and the cytoplasmic vesicles, megalin expression was higher in patients with microalbuminuric IgAN and nonalbuminuric TMD than in controls ( $P < 0.05$ , Figure 5A and C), and cubilin was significantly higher in patients with microalbuminuric IgAN and nonalbuminuric TMD and macroalbuminuric IgAN as compared with controls ( $P < 0.01$ , Figure 5B and 5D). We also found significantly higher expression of megalin and cubilin in the cytoplasmic vesicles than in the brush border in all groups.

### Proximal Tubular Epithelial Megalin and Cubilin in Response to Induced Proteinuria in Zebrafish

At 1 dpf, morphants did not show a global developmental defect. However, at 4 dpf, *nphs2* morphants



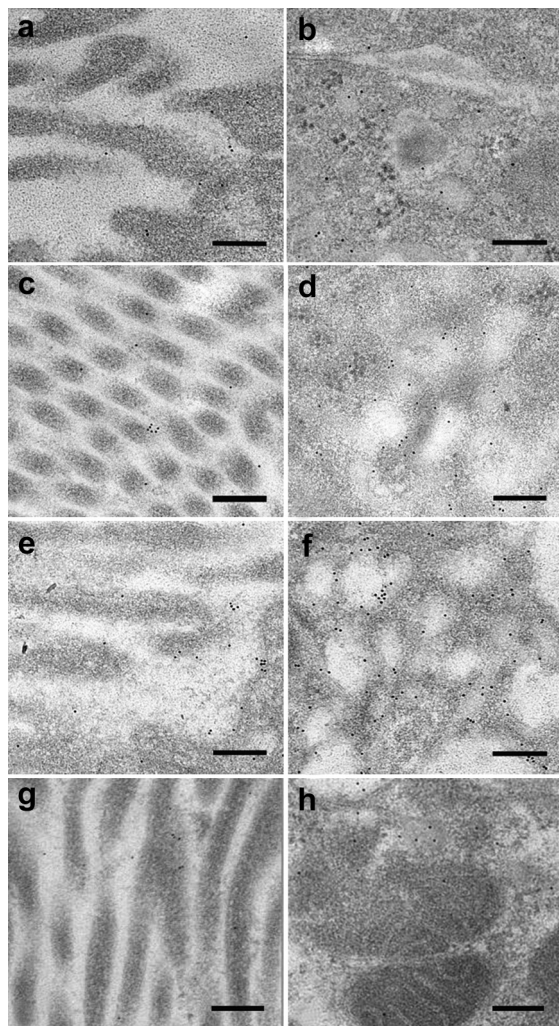


**Figure 3.** Immunoelectron microscopy images of megalin expression. Images are from IgA nephropathy (IgAN) patients with microalbuminuria (<300 mg/24 hours), macroalbuminuria (>300 mg/24 hours and <3500 mg/24 hours), nephrotic-albuminuria (>3500 mg/24 hours), and controls. The different expression of megalin between the 3 groups is shown in the brush border (left panel) of the proximal tubular cells and in the cytoplasm area (right panel) (original magnification  $\times 39,000$ ). Images (a) and (b) show nephrotic-albuminuric IgAN, (c) and (d) show macroalbuminuric IgAN, (e) and (f) show those with microalbuminuria, and (g) and (h) show controls. Note the increased labeling between the 3 groups. Bar = 200 nm.

developed typical pericardial edema (Figure 6A) that appeared to be dose dependent with regard to penetrance and severity (almost 56% of 121 morphants injected with 100  $\mu\text{M}$  MO and 18% of 82 morphants with 50  $\mu\text{M}$  MO). Injection with control MO in zebrafish embryos did not lead to any discernable pericardial edema and these larvae appeared similar to wild-type ones during the observed period.

In the high-dose (100  $\mu\text{M}$ ) *nphs2* morphants, transmission electron microscopy demonstrated severe widespread effacement of podocyte foot processes (Figure 6B[b]), suggesting a structural alteration of the zebrafish model similar to human nephrotic syndrome.

The signal intensity of the albumin-like protein in proximal tubules of *nphs2* morphants (100  $\mu\text{M}$ ) was significantly higher with an almost 4-fold increase than the control ( $P < 0.01$ , Figure 4A), supporting that the zebrafish model is proteinuric. However, low-dose MO (50  $\mu\text{M}$ ) did not lead to significant uptake of plasma protein in the tubules.

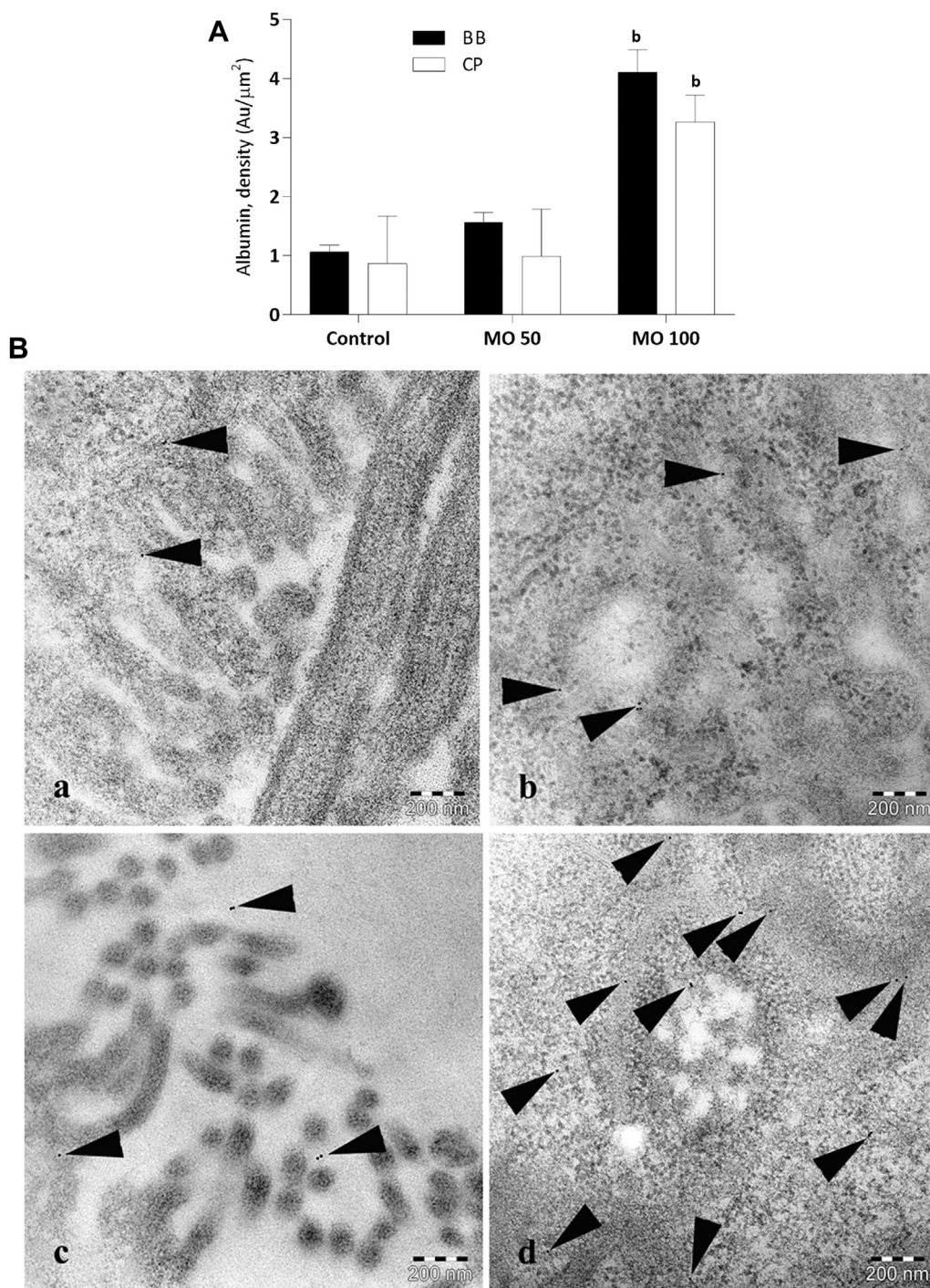
### Semiquantitative Evaluation of Immunoreactive Megalin, Cubilin, and Albumin-like Protein in Proximal Tubular Cells Using iEM in Zebrafish

Figure 7 shows that in proximal tubules of 4-dpf high-dose (100  $\mu\text{M}$ ) morphant, the expression of megalin and cubilin was significantly upregulated with an almost 3-fold and 2-fold increase as compared with the controls ( $P < 0.01$  for both). In addition, megalin appeared to be more sensitive in response to plasma protein uptake than cubilin, because its expression in high-dose *nphs2* morphants was also significantly higher than in low-dose *nphs2* morphants ( $P < 0.05$ ), a trend not observed in cubilin.

## DISCUSSION

To our knowledge, the present study is the first to compare the expression and subcellular localization of megalin and cubilin in proximal tubular epithelial cells from patients with common human kidney diseases. Using iEM, we studied the expression of megalin and cubilin in biopsies from patients with different levels of albuminuria, healthy controls, and proteinuric zebrafish. We report that, compared with healthy donors (negative controls), all patients had elevated amounts of intracellular cubilin. Patients with microalbuminuric IgAN and nonalbuminuric TMD had elevated amounts of brush border and intracellular megalin, a pattern also found in the proteinuric zebrafish. Surprisingly, the highest levels of megalin and cubilin in the brush border and cytoplasmic vesicles were found in nonalbuminuric TMD patients. As no major differences were seen between diagnostic groups (data not shown), our findings suggest but cannot prove that the tubular plasma protein is a key determinant of megalin and cubilin levels in the proximal tubules. Meanwhile, the elevated megalin in nonalbuminuric TMD patients may indicate that protein across the glomerular filter is compensated by tubular reuptake.

In the present study, patients with micro- and macroalbuminuria exhibited elevated cubilin in brush border and cytoplasmic vesicles by both IHC and iEM as compared with controls. All patients had elevated cubilin in cytoplasmic vesicles. There were no differences between controls and nephrotic or macroalbuminuric patients for megalin, but it was elevated in the microalbuminuric IgAN and nonalbuminuric TMD



**Figure 4.** Semiquantification of immunogold-labeled albumin-like protein in proximal tubules of zebrafish. (A) Bar graph illustrates semiquantitative data of protein uptake in proximal tubules. Statistically, (b) denotes results significantly different from controls ( $P < 0.01$ ). (B) Immunoelectron microscopy images showing gold-labeled albumin-like protein (arrowheads) in controls (a, b) and in *nphs2* morphants injected with 100 μM of MO (c, d) in the brush border (left panel) and cytoplasmic vesicles (right panel), respectively ( $\times 60,000$ ). Bar = 200 nm. MO, morpholino antisense oligo.

patients. This finding was observed by Wilmer *et al.*<sup>47</sup> in low-molecular-weight proteinuria patients with cystinosis. In the present study, we add iEM data on several common diagnoses. There are 2 reasons that studies relied on IHC making accurate quantification difficult; one is that the intensity is heterogeneous between biopsies, and furthermore, the intensity is

varying between sections even on the same glass. Therefore, we evaluated biopsies embedded in Lowicryl resin at the EM level using semiquantification of immune-gold-labeled antibodies.

Cell<sup>48</sup> and animal<sup>18,20</sup> studies have previously shown that cubilin is primarily responsible for the normal proximal tubular reuptake of albumin. Amsellem



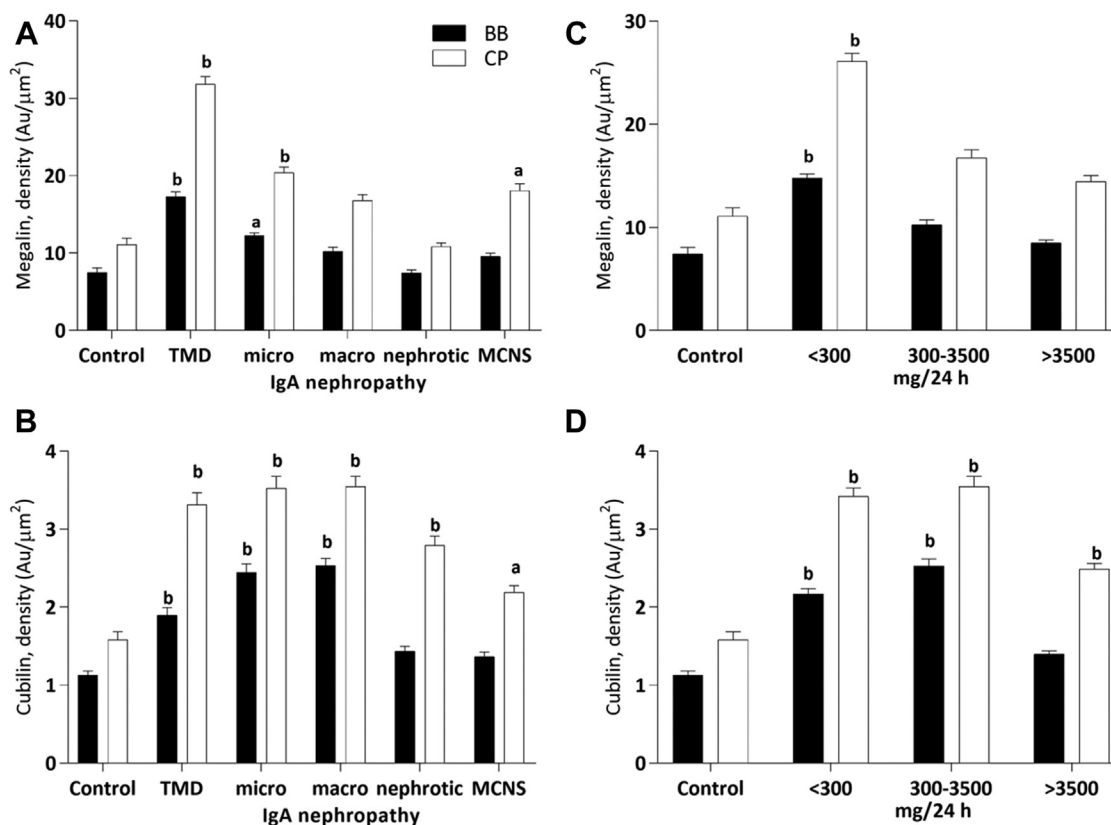


**Figure 5.** Semiquantification of immunogold-labeled (A, C) megalin and (B, D) cubilin. Left panel (A and B) shows that all patients classified by diagnosis—thin membrane disease (TMD), IgA nephropathy (IgAN) with microalbuminuria (<300 mg/24 hours, micro-IgAN), IgAN with macroalbuminuria (>300 mg/24 hours and <3500 mg/24 hours, macro-IgAN), IgAN with nephrotic-albuminuria (>3500 mg/24 hours, nephro-IgAN), and minimal change nephropathy (MCNS)—were compared with living donors (controls) in the proximal tubular brush border (BB) and the cytoplasm area (CP). Right panel (C, D) shows all patients classified by degree of albuminuria—group 1 (albuminuria <300 mg/24 hours) including microalbuminuric IgAN and nonalbuminuric TMD, group 2 (albuminuria >300 mg/24 hours and <3500 mg/24 hours) including macroalbuminuric IgAN, and group 3 (albuminuria >3500 mg/24 hours) including nephrotic-albuminuric IgAN and MCNS—were compared with living donors (controls) in the proximal tubular brush border and the cytoplasm area. Statistically, (a) denotes results different from controls ( $P < 0.05$ ), and (b) denotes results significantly different from controls ( $P < 0.01$ ).

*et al.*<sup>18</sup> even suggested that albumin reabsorption in the tubules was mediated essentially by cubilin. However, they also proposed that the megalin may mediate the internalization of the cubilin-albumin complex. As our studies indicate that megalin is more abundant in the brush border of tubules with low grade albuminuria, it may also play a role during increased protein across the glomerular barrier.<sup>49</sup> Our study is nonconclusive, but we observed lower staining in highly albuminuric tubules; one may speculate that a protective down-regulation of megalin occurs in this setting.

We believed that the expression pattern of megalin and cubilin in response to plasma protein uptake is a physiologically conserved mechanism rather than a chance finding. Therefore, we used a proteinuric zebrafish model to extend our findings in human data. A similar expression pattern in the zebrafish model strengthens the proposed mechanistic link between the tubular plasma protein and levels of megalin and cubilin. We observed a dose-dependent increase of the

plasma protein uptake due to glomerular damage, and this in turn resulted in an increased expression of megalin and cubilin at the higher dose of the morpholinos. These findings may suggest that it is the tubular plasma protein leading to expression alteration of proximal tubular megalin and cubilin.

In both *in vitro* and animal models of tubular protein overload, endocytosis through the megalin and cubilin receptor complex triggers tubulointerstitial inflammation, fibrosis, and tubular apoptosis.<sup>50</sup> The mechanisms remain unknown, but presumably involve the induction of proinflammatory signaling that in turn may be linked to mitochondrial dysfunction.<sup>15,51</sup> However, a study<sup>19</sup> of glomerular proteinuria in a transgenic mouse model with mosaic knockout of *Lrp2* (megalin) found that although the presence of elevated amounts of protein in the proximal tubules did lead to an upregulation of profibrotic mediators in a megalin-dependent way, there was no difference in tubulointerstitial damage between tubules expressing megalin and those that did not. Similar



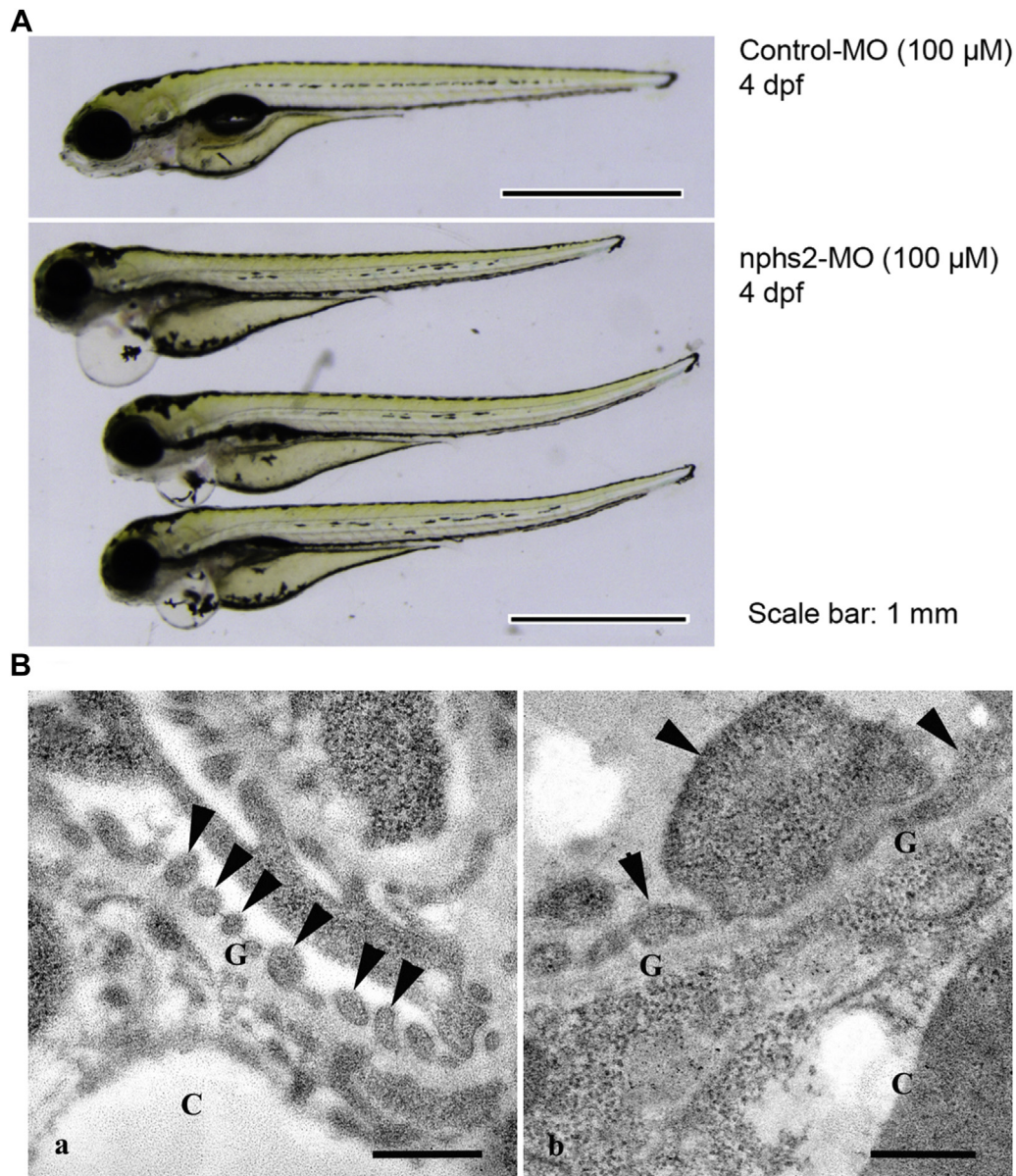


**Figure 6.** Proteinuric zebrafish model. (A) Phenotype of control (larvae injected with control MO) and *nphs2* morphants at 4 days postfertilization (dpf). *Nphs2* morphants develop severe late-stage pericardial edema at 4 dpf, often indicating glomerular injury of pronephros. (B) Ultrastructural alteration of 4-dpf zebrafish glomerular podocytes. (a) Controls show fine and regular podocyte foot processes (arrowheads); (b) *nphs2* morphants display extensive and irregular podocyte foot processes (arrowheads). Bar (A) = 1 mm, (B) = 500 nm. C, capillary lumen; G, glomerular basement membrane; MO, morpholino antisense oligo.

results have been reported in crescentic-nephritic mice, where the lack of megalin in the proximal tubules could not prevent tubulointerstitial injury. Thus, the role of megalin and cubilin expression in the development in interstitial fibrosis is still unclear.

Although, to our knowledge, this study is the first investigation of megalin and cubilin in human albuminuric diseases, the study design suffers from limitations. First, as this is a cross-sectional study on human biopsies, sequential biopsies and the study of chronological effects, including the effect of lowering albuminuria (e.g., with angiotensin receptor blockers), on megalin and cubilin could not be investigated.

Second, all biopsies from human beings used in our study are all from clinical pathology diagnostic biopsies. Following the routine guideline, each biopsy was examined and separated for immunofluorescence microscopy, light microscopy, and transmission electron microscopy, which is mentioned previously. If the biopsy was big enough, a small cortical piece was prospectively prepared for iEM; therefore, there is a possibility that 1 nephron was investigated more than once. Also, we only investigated binding of labeled antibodies using immune-electron microscopy, which does not conclusively prove the presence of functional protein or say anything about actual transcription

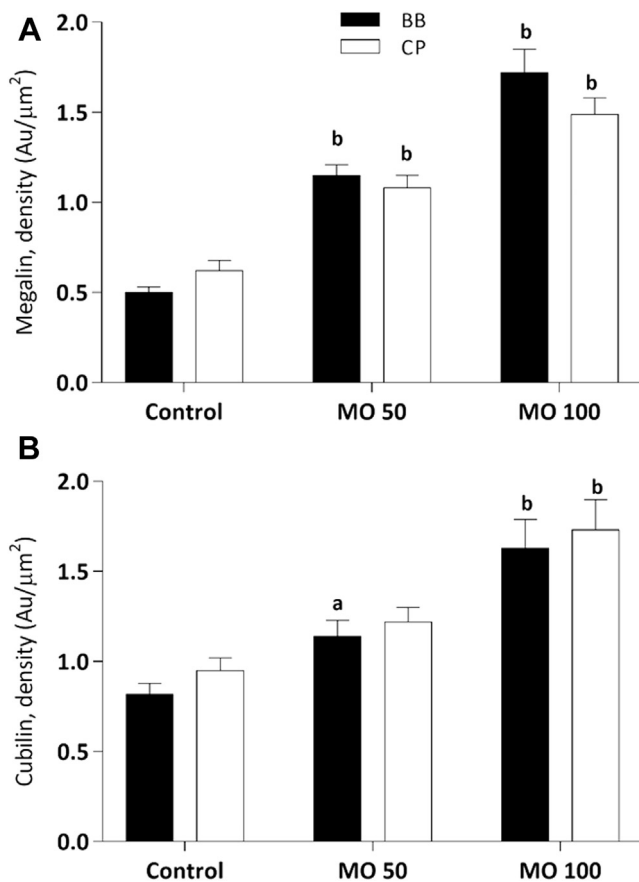


**Figure 7.** Semiquantification of immunogold-labeled (A) megalin and (B) cubilin in the proximal tubular brush border (BB) and the cytoplasmic area (CP) in zebrafish. Statistically, (a) indicates  $P < 0.05$  and (b) indicates  $P < 0.01$  between group and controls (original magnification  $\times 43,000$ ). MO, morpholino antisense oligo.

levels. Finally, although unlikely, it is possible that constitutional limitations in expression or function of one or both of the studied receptors predispose certain individuals to high albuminuria, rather than the number of receptors reflecting albuminuria due to other causes.

In summary, we identified megalin and cubilin in brush border and cytoplasmic vesicles of proximal tubular cells, and the expression patterns in human renal biopsies, as well as in proteinuric zebrafish. In the human renal diseases studied, megalin expression increased in microalbuminuric IgAN and non-albuminuric TMD, whereas cubilin expression increases in all patient groups compared with controls. These findings suggest that megalin and cubilin differentially cooperate in cleaning up the plasma protein in kidney tubules.

## DISCLOSURE

A summary of the findings in this study was presented at the American Society of Nephrology Kidney Week in San Diego, CA, USA, 30 October to 4 November 2012. JA is

the recipient of grants from the Swedish Research Council (no. 2012-1610) and the Swedish Heart and Lung Fund (no. 20130242, 20130267). AW received financial support through the Regional Agreement on Medical Training and Clinical Research (ALF) between Stockholm County Council and Karolinska Institute. The authors declare that they have no other relevant financial interests.

## ACKNOWLEDGMENTS

We thank the dedicated staff at the nephrology and pathology units at Karolinska University Hospital. We are indebted to Professor Renata Kozyraki, Institute de la Vision, INSERM, Paris, France, for the gift of megalin and cubilin antibodies; Abdul Rashid Qureshi for help with the statistical analysis; the Kidney-KBC (consulting and treatment center) research unit at Karolinska University Hospital for assistance with urine and blood tests; and Ingrid Lindell and Eva Blomén for skillful technical assistance.

## REFERENCES

1. Kerjaschki D, Farquhar MG. The pathogenic antigen of Heymann nephritis is a membrane glycoprotein of the renal proximal tubule brush border. *Proc Natl Acad Sci USA*. 1982;79:5557-5561.
2. Sahali D, Mulliez N, Chatelet F, et al. Characterization of a 280-kD protein restricted to the coated pits of the renal brush border and the epithelial cells of the yolk sac. Teratogenic effect of the specific monoclonal antibodies. *J Exp Med*. 1988;167:213-218.
3. Christensen EI, Birn H. Megalin and cubilin: multifunctional endocytic receptors. *Nat Rev Mol Cell Biol*. 2002;3:256-266.
4. Tanner GA. Renal physiology and body fluids, kidney function. In: Rhodes R, Bell D, eds. *Medical Physiology: Principles for Clinical Medicine. Third Edition*. Baltimore and Philadelphia: Lippincott Williams & Wilkins; 2009:391-418.
5. Storm T, Tranebjærg L, Frykholm C, et al. Renal phenotypic investigations of megalin-deficient patients: novel insights into tubular proteinuria and albumin filtration. *Nephrol Dial Transplant*. 2013;28:585-591.
6. Christensen EI, Birn H, Verroust P, Moestrup SK. Membrane receptors for endocytosis in the renal proximal tubule. *Int Rev Cytol*. 1998;180:237-284.
7. Anzenberger U, Bit-Avrágim N, Rohr S, et al. Elucidation of megalin/LRP2-dependent endocytic transport processes in the larval zebrafish pronephros. *J Cell Sci*. 2006;119:2127-2137.
8. Tojo A, Onozato ML, Kitiyakara C, et al. Glomerular albumin filtration through podocyte cell body in puromycin aminonucleoside nephrotic rat. *Med Mol Morphol*. 2008;41:92-98.
9. Comper WD, Glasgow EF. Charge selectivity in kidney ultrafiltration. *Kidney Int*. 1995;47:1242-1251.
10. Gekle M. Renal tubule albumin transport. *Annu Rev Physiol*. 2005;67:573-594.
11. Cravedi P, Remuzzi G. Pathophysiology of proteinuria and its value as an outcome measure in chronic kidney disease. *Br J Clin Pharmacol*. 2013;76:516-523.



12. Lazzara MJ, Deen WM. Model of albumin reabsorption in the proximal tubule. *Am J Physiol Renal Physiol.* 2007;292:F430–F439.
13. Eddy AA. Proteinuria and interstitial injury. *Nephrol Dial Transplant.* 2004;19:277–281.
14. Tojo A, Kinugasa S. Mechanisms of glomerular albumin filtration and tubular reabsorption. *Int J Nephrol.* 2012;2012:481520.
15. Erkan E, Devarajan P, Schwartz GJ. Mitochondria are the major targets in albumin-induced apoptosis in proximal tubule cells. *J Am Soc Nephrol.* 2007;18:1199–1208.
16. Nielsen R, Birn H, Moestrup SK, et al. Characterization of a kidney proximal tubule cell line, LLC-PK1, expressing endocytotic active megalin. *J Am Soc Nephrol.* 1998;9:1767–1776.
17. Li Y, Cong R, Biemesderfer D. The COOH terminus of megalin regulates gene expression in opossum kidney proximal tubule cells. *Am J Physiol Cell Physiol.* 2008;295:C529–C537.
18. Amsellem S, Gburek J, Hamard G, et al. Cubilin is essential for albumin reabsorption in the renal proximal tubule. *J Am Soc Nephrol.* 2010;21:1859–1867.
19. Theilig F, Kriz W, Jerichow T, et al. Abrogation of protein uptake through megalin-deficient proximal tubules does not safeguard against tubulointerstitial injury. *J Am Soc Nephrol.* 2007;18:1824–1834.
20. Weyer K, Storm T, Shan J, et al. Mouse model of proximal tubule endocytic dysfunction. *Nephrol Dial Transplant.* 2011;26:3446–3451.
21. Leheste JR, Rolinski B, Vorum H, et al. Megalin knockout mice as an animal model of low molecular weight proteinuria. *Am J Pathol.* 1999;155:1361–1370.
22. Odera K, Goto S, Takahashi R. Age-related change of endocytic receptors megalin and cubilin in the kidney in rats. *Biogerontology.* 2007;8:505–515.
23. Morales CR, Igdoura SA, Wosu UA, et al. Low density lipoprotein receptor-related protein-2 expression in efferent duct and epididymal epithelia: evidence in rats for its in vivo role in endocytosis of apolipoprotein J/clusterin. *Biol Reprod.* 1996;55:676–683.
24. Vinge L, Lees GE, Nielsen R, et al. The effect of progressive glomerular disease on megalin-mediated endocytosis in the kidney. *Nephrol Dial Transplant.* 2010;25:2458–2467.
25. Fyfe JC, Ramanujam KS, Ramaswamy K, et al. Defective brush-border expression of intrinsic factor-cobalamin receptor in canine inherited intestinal cobalamin malabsorption. *J Biol Chem.* 1991;266:4489–4494.
26. Melilli E, Cruzado JM, Bestard O, Hernández D. Mechanisms and risk factors for the development of the proteinuria after kidney transplantation. *Transplant Rev (Orlando).* 2012;26:14–19.
27. Nielsen R, Christensen EI, Birn H. Megalin and cubilin in proximal tubule protein reabsorption: from experimental models to human disease. *Kidney Int.* 2016;89:58–67.
28. Bökenkamp A, Ludwig M. Disorders of the renal proximal tubule. *Nephron Physiol.* 2011;118:p1–p6.
29. Norden AG, Lapsley M, Igarashi T, et al. Urinary megalin deficiency implicates abnormal tubular endocytic function in Fanconi syndrome. *J Am Soc Nephrol.* 2002;13:125–133.
30. Gorvin CM, Wilmer MJ, Piret SE, et al. Receptor-mediated endocytosis and endosomal acidification is impaired in proximal tubule epithelial cells of Dent disease patients. *Proc Natl Acad Sci USA.* 2013;110:7014–7019.
31. Dachy A, Paquot F, Debray G, et al. In-depth phenotyping of a Donnai-Barrow patient helps clarify proximal tubule dysfunction. *Pediatr Nephrol.* 2015;30:1027–1031.
32. Kantarci S, Ragge NK, Thomas NS, et al. Donnai-Barrow syndrome (DBS/FOAR) in a child with a homozygous LRP2 mutation due to complete chromosome 2 paternal isodisomy. *Am J Med Genet A.* 2008;146A:1842–1847.
33. Kantarci S, Al-Gazali L, Hill RS, et al. Mutations in LRP2, which encodes the multiligand receptor megalin, cause Donnai-Barrow and facio-oculo-acoustico-renal syndromes. *Nat Genet.* 2007;39:957–959.
34. Donnai D, Barrow M. Diaphragmatic hernia, exomphalos, absent corpus callosum, hypertelorism, myopia, and sensorineural deafness: a newly recognized autosomal recessive disorder? *Am J Med Genet.* 1993;47:679–682.
35. Namour F, Dobrovoljski G, Chery C, et al. Luminal expression of cubilin is impaired in Imerlund-Grasbeck syndrome with compound AMN mutations in intron 3 and exon 7. *Haematologica.* 2011;96:1715–1719.
36. Storm T, Emma F, Verroust PJ, et al. A patient with cubilin deficiency. *N Engl J Med.* 2011;364:89–91.
37. Aminoff M, Carter JE, Chadwick RB, et al. Mutations in CUBN, encoding the intrinsic factor-vitamin B12 receptor, cubilin, cause hereditary megaloblastic anaemia 1. *Nat Genet.* 1999;21:309–313.
38. Storm T, Zeitz C, Cases O, et al. Detailed investigations of proximal tubular function in Imerlund-Gräsbeck syndrome. *BMC Med Genet.* 2013;14:111.
39. Mihout F, Devuyt O, Bensman A, et al. Acute metabolic acidosis in a GLUT2-deficient patient with Fanconi-Bickel syndrome: new pathophysiology insights. *Nephrol Dial Transplant.* 2014;29(suppl 4):iv113–iv116.
40. Toto RD. Microalbuminuria: definition, detection, and clinical significance. *J Clin Hypertens (Greenwich).* 2004;6:2–7.
41. Vivian EM. Endocrine disorders. In: Lee M, ed. *Basic Skills in Interpreting Laboratory Data, 4th edition.* Bethesda: American Society of Health-System Pharmacists; 2009:291.
42. Kramer-Zucker AG, Wiessner S, Jensen AM, Drummond IA. Organization of the pronephric filtration apparatus in zebrafish requires nephrin, podocin and the FERM domain protein Mosaic eyes. *Dev Biol.* 2005;285:316–329.
43. Akimenko MA, Johnson SL, Westerfield M, Ekker M. Differential induction of four msx homeobox genes during fin development and regeneration in zebrafish. *Development.* 1995;121:347–357.
44. Noël ES, Reis MD, Arain Z, Ober EA. Analysis of the albumin/alpha-fetoprotein/afamin/group specific component gene family in the context of zebrafish liver differentiation. *Gene Expr Patterns.* 2010;10:237–243.
45. Wernerson A, Dunér F, Pettersson E, et al. Altered ultrastructural distribution of nephrin in minimal change

- nephrotic syndrome. *Nephrol Dial Transplant*. 2003;18:70–76.
46. Weibel ER. *Practice Methods for Biological Morphometry*. London: Academic Press; 1979.
  47. Wilmer MJ, Christensen EI, van den Heuvel LP, et al. Urinary protein excretion pattern and renal expression of megalin and cubilin in nephropathic cystinosis. *Am J Kidney Dis*. 2008;51:893–903.
  48. Zhai XY, Nielsen R, Birn H, et al. Cubilin- and megalin-mediated uptake of albumin in cultured proximal tubule cells of opossum kidney. *Kidney Int*. 2000;58:1523–1533.
  49. Briffa JF, Grinfeld E, Poronnik P, et al. Uptake of leptin and albumin via separate pathways in proximal tubule cells. *Int J Biochem Cell Biol*. 2016;79:194–198.
  50. Zoja C, Donadelli R, Colleoni S, et al. Protein overload stimulates RANTES production by proximal tubular cells depending on NF-kappa B activation. *Kidney Int*. 1998;53:1608–1615.
  51. Nishi Y, Satoh M, Nagasu H, et al. Selective estrogen receptor modulation attenuates proteinuria-induced renal tubular damage by modulating mitochondrial oxidative status. *Kidney Int*. 2013;83:662–673.